TESTING THE ACCURACY OF DIFFERENT LIDAR SCANNING STRATEGIES WITH LARGE-EDDY SIMULATIONS

Maggie McMahon[1], Joshua Gebauer[2], and Jeremy Gibbs[3]

[1]National Weather Center Research Experiences for Undergraduates Program
Norman, Oklahoma
[2]Cooperative Institute for Severe and High-Impact Weather Research and Operations, NOAA National Severe Storms Laboratory, University of Oklahoma
Norman, Oklahoma
[3]NOAA National Severe Storms Laboratory
Norman, Oklahoma

ABSTRACT

Lidar scans can obtain data with high temporal resolution but they can only measure radial velocities, which can lead to inaccurate measurements for wind velocities and turbulence. To improve the performance of future lidar scans in various environments, this study collected data on the accuracy of different scanning strategies' retrievals under particular wind conditions. A virtual lidar took measurements from the output of large-eddy simulations with different initial vertical wind shears, using a variety of scanning techniques whose results were compared. The retrievals from each scan were used to calculate the component winds and variances, which were then analyzed on how closely they matched the true wind values of the simulations. The scanning strategies tested were different Doppler beam swinging (DBS) and velocity-azimuth display (VAD) scans with modified elevation angles and numbers of beams, as well as the six-beam method. The scans were judged based on the mean and instantaneous root-mean-square errors (RMSEs) between their observations and the actual winds. While there is no single scanning strategy that always got the best results for every wind component, the 8-point VAD with a vertical beam method got the best average wind velocity and turbulence results, and the VAD scans overall did a better job than the DBS scans. Additionally, techniques that were tested with multiple elevation angles got the most consistently accurate wind observations from scans done at 60° and 50°. The findings also show that it is difficult to measure vertical velocity variance accurately unless the lidar scan includes a 90° beam.

1. INTRODUCTION

A lidar is a remote sensing device that transmits beams of light to detect atmospheric aerosols. The Doppler shift in the return signal is used to measure the line-of-sight (LOS) velocity of the aerosol targets that scattered the beam, which can be assumed to also be the LOS velocity of the wind carrying those aerosols. By observing the radial wind velocities, lidars can measure horizontal wind velocities and wind turbulences across a 3D volume of the atmosphere. This gives them a spatial advantage over a traditional anemometer or a sonic anemometer, which only measure winds at one point in space. In addition to this, lidars also have a high temporal resolution and can retrieve winds in seconds.

However, since lidars can only measure the component velocity parallel to the transmitted beam, they are unable to directly observe the 3D wind vector; this is why lidars typically operate with different scanning strategies that measure multiple radial velocities with multiple beams in order to retrieve wind profiles. From these measured radial velocities, the lidar then calculates the component winds in the u (east-west, with westerly winds having positive velocity), v (north-south, with southerly winds having positive velocity), and w (up-down, with winds blowing upward having positive velocity) directions to obtain a 3D wind profile.

When these retrievals are used within the scanning area, however, they incorrectly assume that the environment is homogeneous (Menke et

Correspondence to: Maggie McMahon, University of Georgia, 148 Old Will Hunter Rd Apt D07, Athens, GA 30606, Email: msm69048@uga.edu

al. 2020) – which is highly unlikely in real-life situations – and this can lead to errors in the measurements of winds. The errors in wind can also create a false variability which can result in error in variances when lidars are used to measure turbulence.

In this study an experimental approach similar to Robey and Lundquist (2022) is used. Large-eddy simulations (LESs) and a virtual lidar are used to determine the best lidar scanning strategies for measuring winds and turbulence in varying boundary layer conditions.

2. LIDAR SCANNING METHODS

When lidars are used for measuring wind and turbulence, they scan their surroundings in a conical rotation at a specific elevation angle, retrieving winds with height by taking data from a number of points around a circular cross section of the scan at a certain height above the ground. Two widely used lidar scanning techniques are the Doppler beam swinging (DBS) and velocity-azimuth display (VAD) scans (Newman et al. 2016). A DBS scan retrieves measurements from just four points around the scan circle, so this method is faster with a higher temporal resolution. A VAD scan measures more than four points, collecting data with a higher spatial resolution but taking longer to finish.

The third scanning method used in this study is the six-beam strategy. This scan measures five data points around the scan circle at an elevation angle of 45° with an additional sixth beam pointed at 90° vertical. Unlike the DBS and VAD scans which calculate wind variance using the retrieved winds, the six-beam method directly calculates the variance from the difference in wind radial velocities over time as measured by each individual beam. The downside of this independent wind variance calculation technique is that it may produce negative, and thus unreal, variance values (Newman et al. 2016).

Every scanning technique and elevation angle combination tried in this experiment can be practiced with a real lidar. By testing different scanning strategies in simulations of specific known wind shears, the data from this experiment can be used to help judge which type of scan should be used under particular wind conditions in real-life situations.

3. DATA AND METHODS

3.1 *LES Model*

In this experiment, a virtual lidar (https://github.com/jgebauer44/LidarSim.git) was run on output from high-resolution large-eddy simulations to simulate a real lidar scanning its surroundings in the boundary layer.

The experiment used the MicroHH 1.0 fluid dynamics code (van Heerwaarden et al. 2017) to simulate typical environments in the boundary layer. The simulations have a domain size of 256 x 256 x 128 with grid spacing of 16 meters. Each simulation was run for a spin-up time of 5 hours and 50 minutes to develop a realistically turbulent boundary layer, then for the 10-minute period running from 5 hours and 50 minutes until 6 hours, the LES output was collected to be scanned by the virtual lidar. Data from the model was gathered every 1 second during this time. The time period for the lidar scan was limited to 10 minutes to keep the file sizes of the simulations manageable. The model output represents the true wind values of each simulated environment. These simulations were set to initial vertical wind shears of zero (with the u component of the geostrophic winds being zero; referred to as UG00), five (UG05), and ten (UG10) meters per second to present environments of differing wind conditions.

3.2 *Virtual Lidar*

To emulate an actual lidar, a virtual lidar coded in Python collected measurements from the output of these models. This virtual lidar has realistic scan timing and beam weighting (Lundquist et al. 2015) in order to copy the behavior of a real lidar as closely as possible. Scan settings including the pulse width and scanning speed of the lidar can be adjusted, and the elevation angles and number of beams used by the lidar can be modified for different scans, as well. In this study, the pulse width and lidar scanning speed were held constant, but the scanning strategies were varied.

The virtual lidar used six scanning strategies to retrieve wind profiles from each simulation. Four of these strategies used the VAD method: an 8-point VAD, a 24-point VAD, an 8-point VAD with an additional 90° beam, and an 18-point VAD that used one virtual lidar in continuous scanning mode (CSM) and one that stared 90° vertical. Two strategies were DBS scans: a regular four-point DBS and a DBS with a vertical beam.

The last strategy tested was the six-beam method. In each simulation, every scanning strategy was repeated at elevation angles of 10°, 20°, 30°, 40°, 50°, 60°, and 70°; except for the six-beam method which always scans at 45°. The data collected by the lidar was then verified against the environment's true wind values as determined by the LES output, in order to check how closely the lidar-measured wind velocities and variances for each scanning strategy matched the actual winds.

To calculate the component winds from a VAD scan, the measured radial velocities over azimuth angle θ of the lidar beam are matched to a cosine curve (Newsom et al. 2019) by minimizing the function:

$$L = \sum_{i=0}^{N-1} (\boldsymbol{u} \cdot \hat{\boldsymbol{r}}_{\boldsymbol{i}} - u_{ri})^2$$

where L is the error term; N is the lidar beam number; $\boldsymbol{u}$ is the velocity vector u, v, or w; $\hat{\boldsymbol{r}}_{\boldsymbol{i}}$ is the vector from the lidar to the point being measured along the beam; and u_{ri} is the measured radial velocity along the beam. The amplitude, phase shift, and offset of the cosine curve are then used to determine wind direction and horizontal and vertical wind speeds, from which u, v, and w are derived.

The DBS scans calculate the u, v, and w component winds from the radial velocities measured by the beams using the following equations (Newman et al. 2016):

$$u = \frac{v_{r2} - v_{r4}}{2cos\phi}$$

$$v = \frac{v_{r1} - v_{r3}}{2cos\phi}$$

$$w = \frac{cos^2\Theta(v_{r1} + v_{r3}) + sin^2\Theta(v_{r2} + v_{r4})}{2sin\phi}$$

where u, v, and w are the wind velocities; v_{rN} is the radial velocity measured by one of the beams with N indicating the number of the beam from one through four in scan order; ϕ is the elevation angle of the beam as measured from the ground; and Θ is the direction of the wind in degrees.

Both the DBS and VAD scanning methods calculate wind variance from the retrieved wind components. The six-beam method uses a different technique, calculating the wind variances directly from the radial velocity variances of the six beams. When scanning with the six-beam strategy, the equations (Newman et al. 2016) used to determine the wind velocity variances in the u, v, and w directions are:

$$u'_{6b}{}^2 = -0.4v'_{r1}{}^2 + 1.05\left(v'_{r2}{}^2 + v'_{r5}{}^2\right) + 0.15\left(v'_{r3}{}^2 + v'_{r4}{}^2\right) - v'_{r6}{}^2$$

$$v'_{6b}{}^2 = 1.2v'_{r1}{}^2 - 0.25\left(v'_{r2}{}^2 + v'_{r5}{}^2\right) + 0.65\left(v'_{r3}{}^2 + v'_{r4}{}^2\right) - v'_{r6}{}^2$$

$$w'_{6b}{}^2 = v'_{r6}{}^2$$

where u'^2, v'^2, and w'^2 are the variances in the u, v, and w directions with the subscript $6b$ distinguishing values that are calculated using the six-beam method; and $v'_{rN}{}^2$ is the radial velocity variance measured by one of the beams with N indicating the number of the beam from one through six in scan order.

3.3 *RMSE Calculations*

Analysis of how well each lidar scan performed was partially based on the root-mean-square errors (RMSEs) of the wind velocities and variances measured by the lidar in comparison to those from the LES output. The RMSEs of each elevation angle of each scanning method were calculated with the equation

$$\mathrm{RMSE} = \sqrt{\frac{\sum_{\mathrm{i}=1}^{\mathrm{n}} \left(\widehat{\mathrm{U}}_{\mathrm{i}} - \mathrm{U}_{\mathrm{i}}\right)^2}{\mathrm{n}}}$$

where U denotes the wind velocity values in the u, v, and w directions as well as the variations u'u', v'v', and w'w' of these values; and the accent $\widehat{\ }$ indicates that a value was measured by the virtual lidar (observed) rather than taken from model output (actual).

This equation was used to calculate both the mean and the instantaneous (i.e., given at each height) deviations of the lidar-measured winds from the winds' actual values. The mean RMSE of every method was calculated by using mean velocity and variance values, and the instantaneous RMSEs were calculated using the retrieved velocity values. The mean RMSEs were used to evaluate how accurately the scan captured the average turbulence characteristics, while the instantaneous RMSEs assessed how well the scans were retrieving the wind profile at

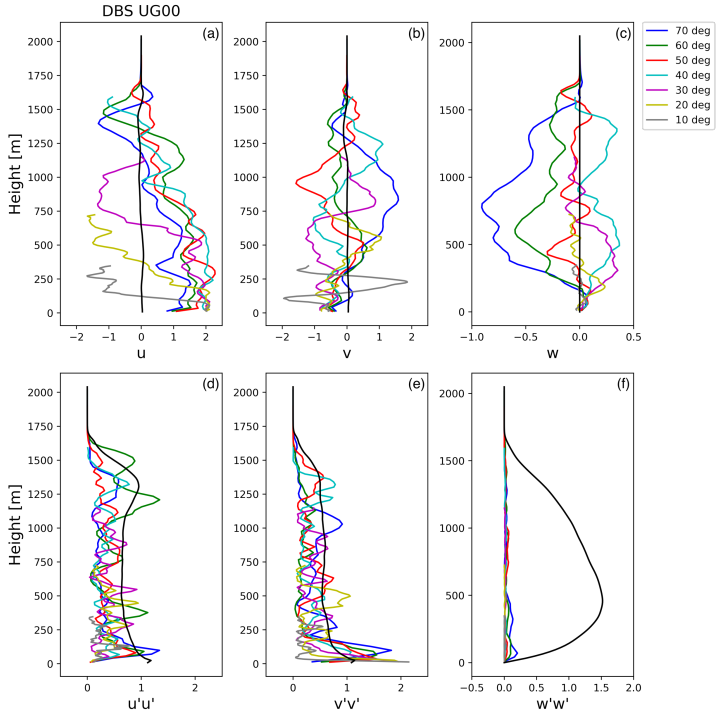
DBS UG00
(a)
(b)
(c)
(d)
(e)
(f)
70 deg
60 deg
50 deg
40 deg
30 deg
20 deg
10 deg
Height [m]
u
v
w
u'u'
v'v'
w'w'

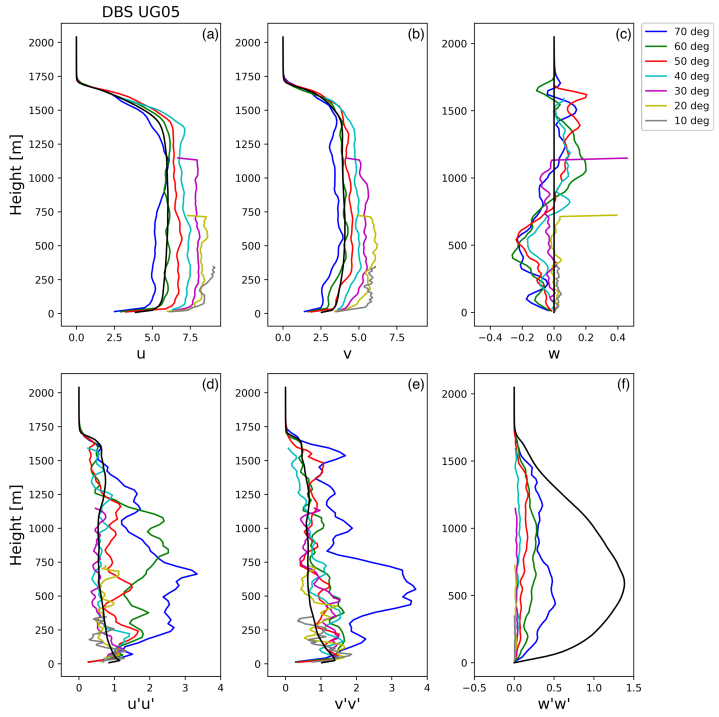
DBS UG05
(a)
(b)
(c)
(d)
(e)
(f)
70 deg
60 deg
50 deg
40 deg
30 deg
20 deg
10 deg
Height [m]
u
v
w
u'u'
v'v'
w'w'

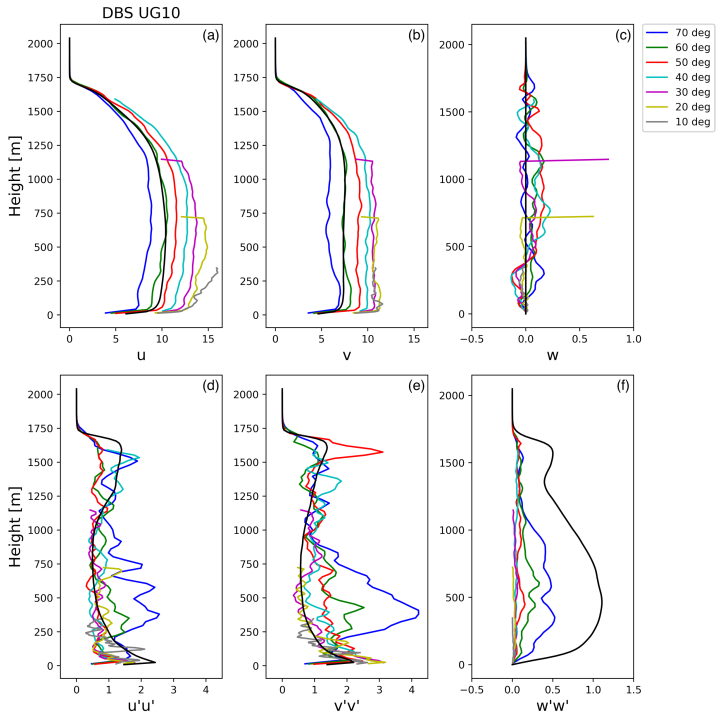

Figure 1. Mean wind velocities and variances measured by the DBS scans at elevation angles 10° through 70° in the UG00, UG05, and UG10 LESs. The LES mean wind is plotted in black. The u wind velocity components are plotted in graphs (a), the v components in graphs (b), and the w components in graphs (c). The u wind variances are plotted in graphs (d), the v variances in graphs (e), and the w variances in graphs (f).

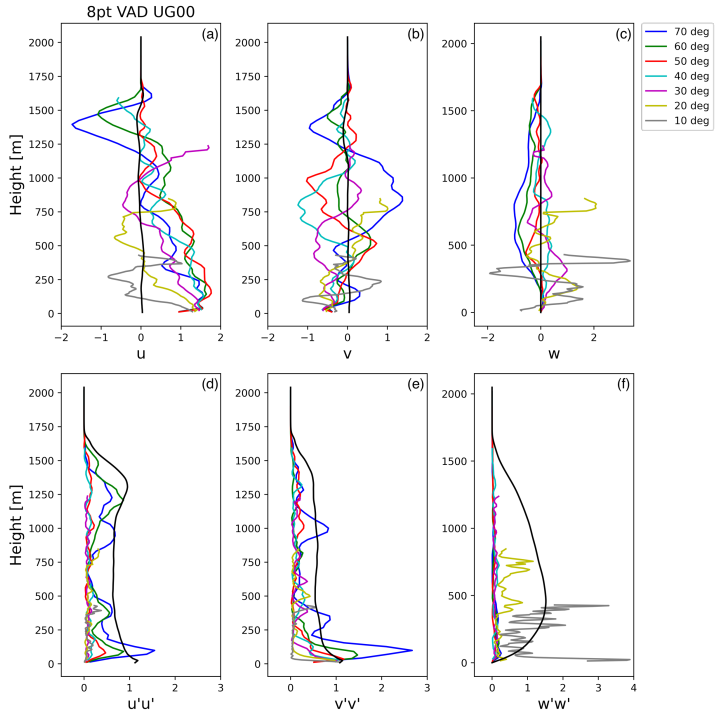

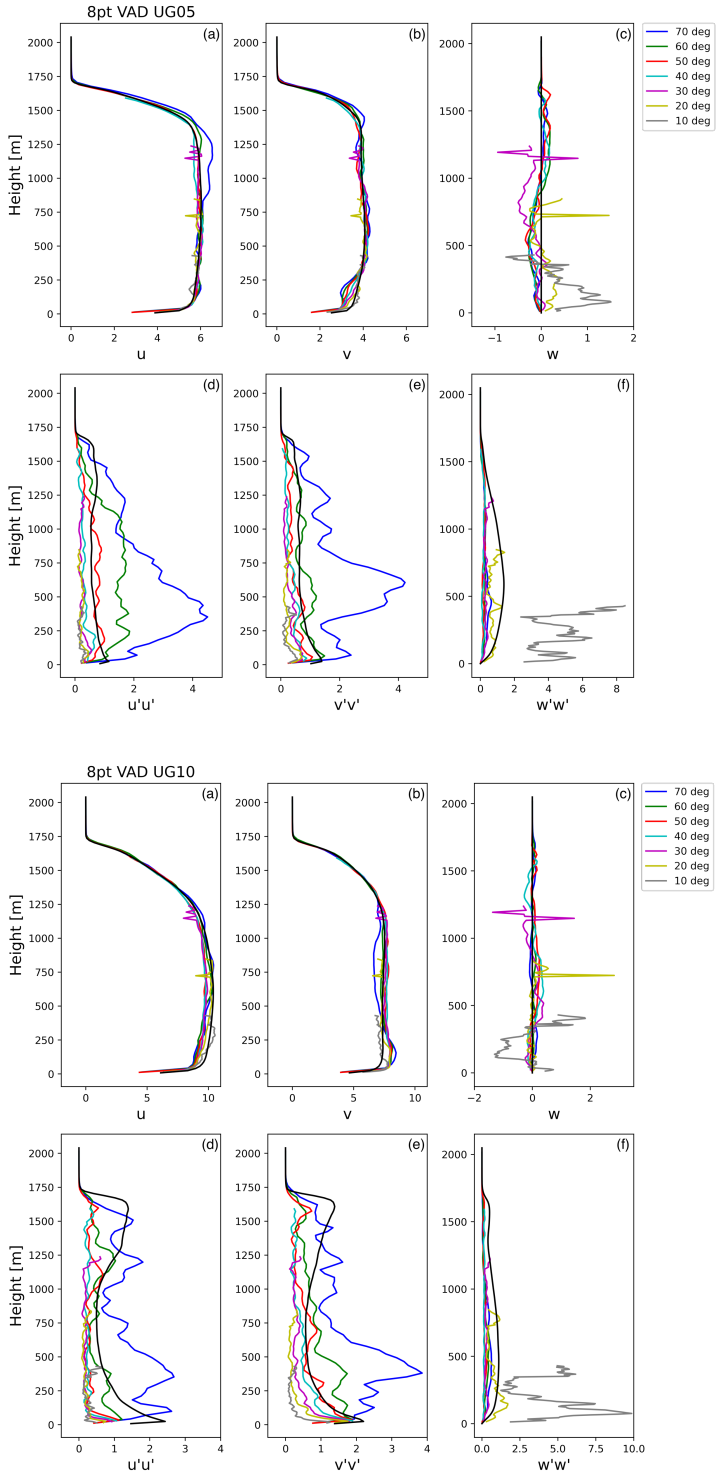

Figure 2. Same values as Fig. 1, but for the 8-point VAD scans.

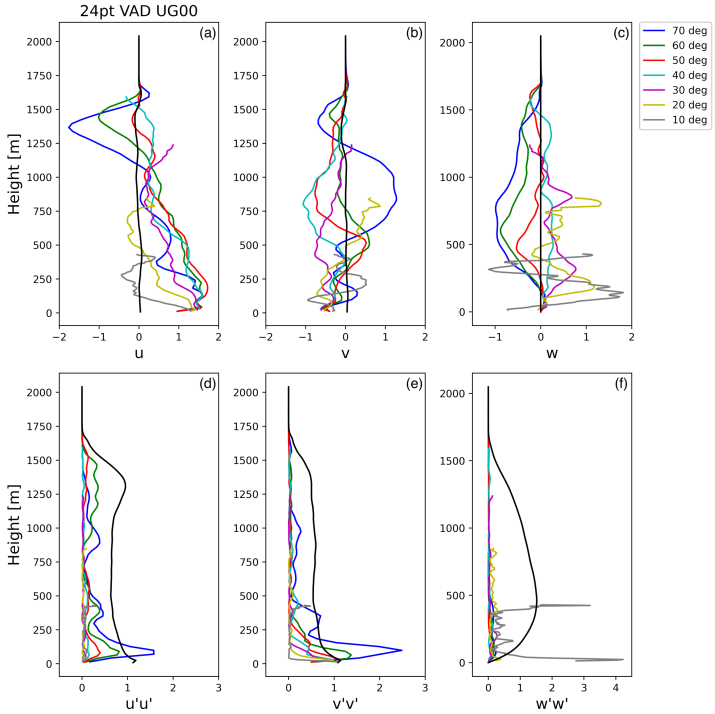
24pt VAD UG00
(a)
(b)
(c)
(d)
(e)
(f)
Height [m]
u
v
w
u'u'
v'v'
w'w'
70 deg
60 deg
50 deg
40 deg
30 deg
20 deg
10 deg

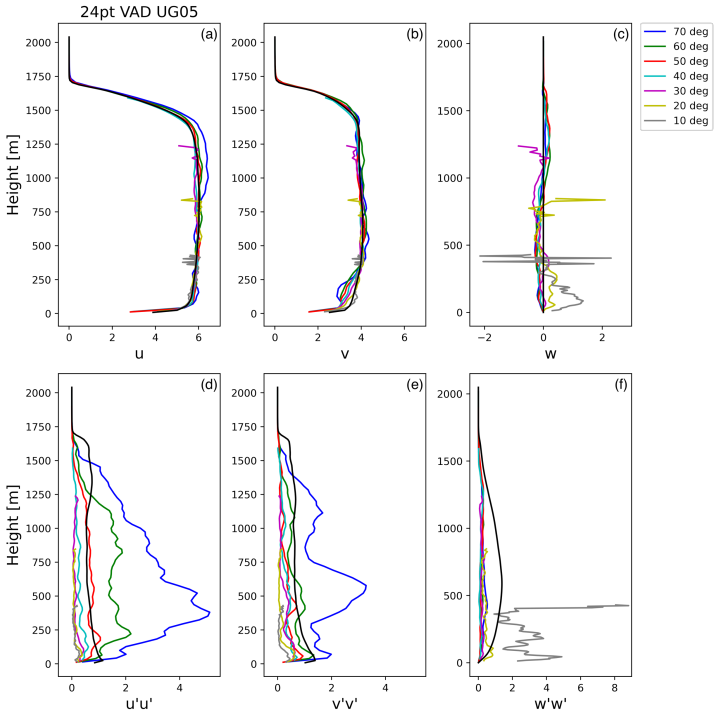
24pt VAD UG05
(a)
(b)
(c)
(d)
(e)
(f)
Height [m]
u
v
w
u'u'
v'v'
w'w'
70 deg
60 deg
50 deg
40 deg
30 deg
20 deg
10 deg

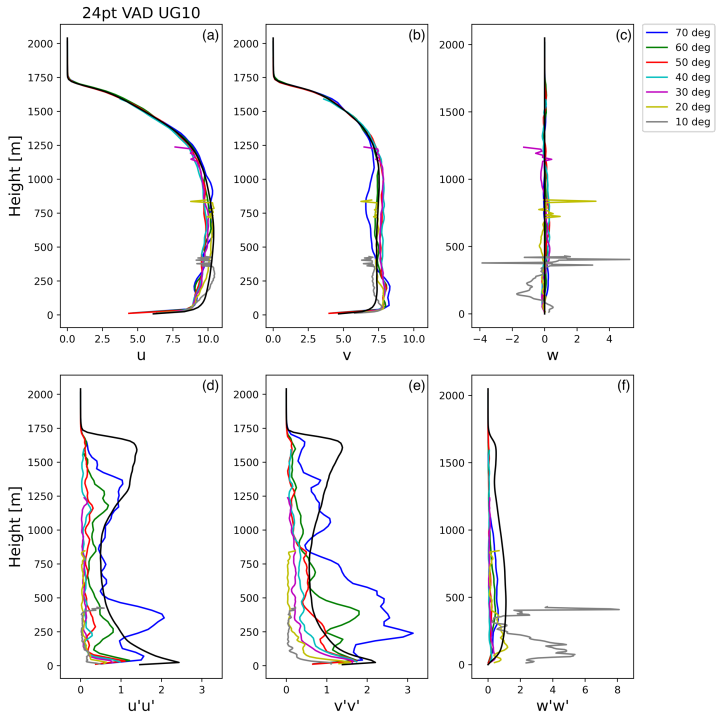

Figure 3. Same values as Fig. 1, but for the 24-point VAD scans.

the lidar location. Using both RMSEs allows one to determine if the variance calculations are dominated by wind retrieval error.

4. RESULTS AND DISCUSSION

4.1 *Mean Winds and Variances*

The mean wind velocities as well as the wind variances over height in the component u, v, and w directions that were retrieved by the lidar for the DBS, 8-point VAD, and 24-point VAD scans can be seen in Figures 1–3. The true mean wind values as given by the LES model outputs are plotted in black for comparison. The performance of each scanning technique, in every wind shear environment and at all the elevation angles as outlined in the methods section above, was assessed based on the difference between the observed values and the actual winds.

The UG05 LES got the most accurate general results from all scanning strategies, followed by the UG10 LES and finally the UG00 LES. Furthermore, the accuracy of the retrievals was greatly affected by the elevation angle of the lidar beam. In the UG00 simulation, the scans done at an angle of 60° were determined to give the observations that were the overall closest match to the actual mean wind velocities and variances, across all three scanning techniques. The 50° and 60° elevation angles performed the best in the UG05 and UG10 environments, respectively. Going forward, only the scans done at these angles will be used to consider the performance of any of the above three scanning strategies in any of the test simulations. The same angles used for the 8-point VAD and DBS will also be used for the 8-point VAD and DBS scans with vertical beams. The 18-point CSM VAD was only tested at an elevation angle of 50° in all three simulations; based on the results from the other VAD scans, this angle was estimated to be the most likely to accurately measure both average wind velocities and average variances.

Figure 4 compares the mean wind retrievals from the best or only elevation angles of each scanning method in the UG00, UG05, and UG10 LESs. Tables 1–3 show the RMSEs calculated for $\overline{u}$, $\overline{v}$, $\overline{w}$, $\overline{u'u'}$, $\overline{v'v'}$, and $\overline{w'w'}$ values averaged over height. These RMSEs were analyzed to help judge how well the scanning methods measured the mean wind and variances.

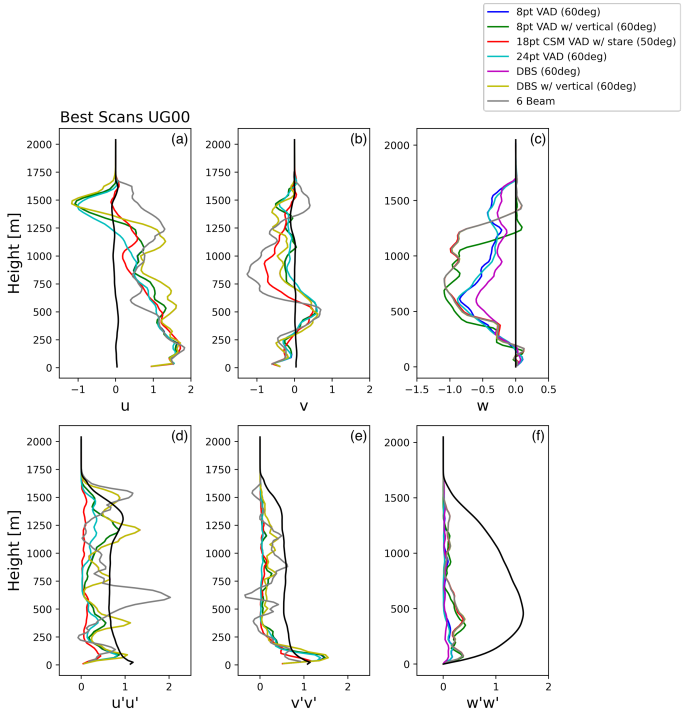
8pt VAD (60deg)
8pt VAD w/ vertical (60deg)
18pt CSM VAD w/ stare (50deg)
24pt VAD (60deg)
DBS (60deg)
DBS w/ vertical (60deg)
6 Beam
Best Scans UG00
(a)
(b)
(c)
(d)
(e)
(f)
Height [m]
u
v
w
u'u'
v'v'
w'w'

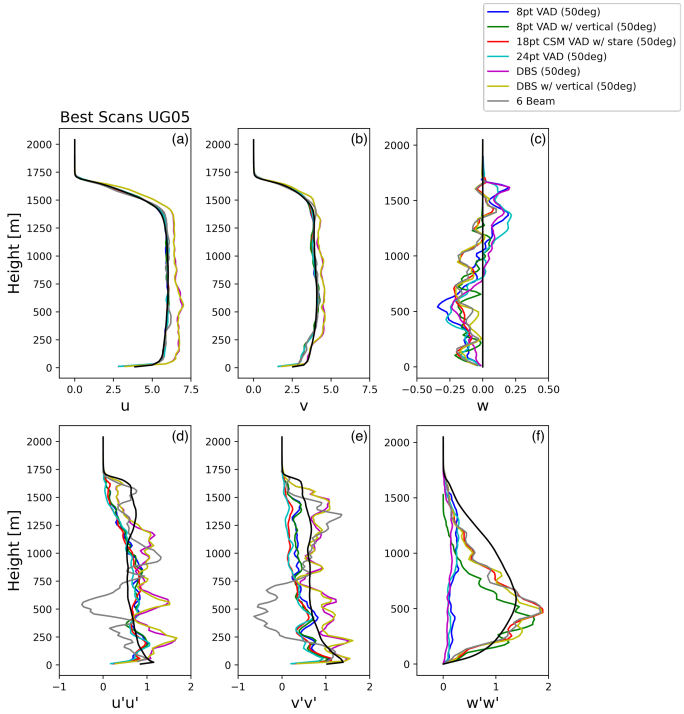
8pt VAD (50deg)
8pt VAD w/ vertical (50deg)
18pt CSM VAD w/ stare (50deg)
24pt VAD (50deg)
DBS (50deg)
DBS w/ vertical (50deg)
6 Beam
Best Scans UG05
(a)
(b)
(c)
(d)
(e)
(f)
Height [m]
u
v
w
u'u'
v'v'
w'w'

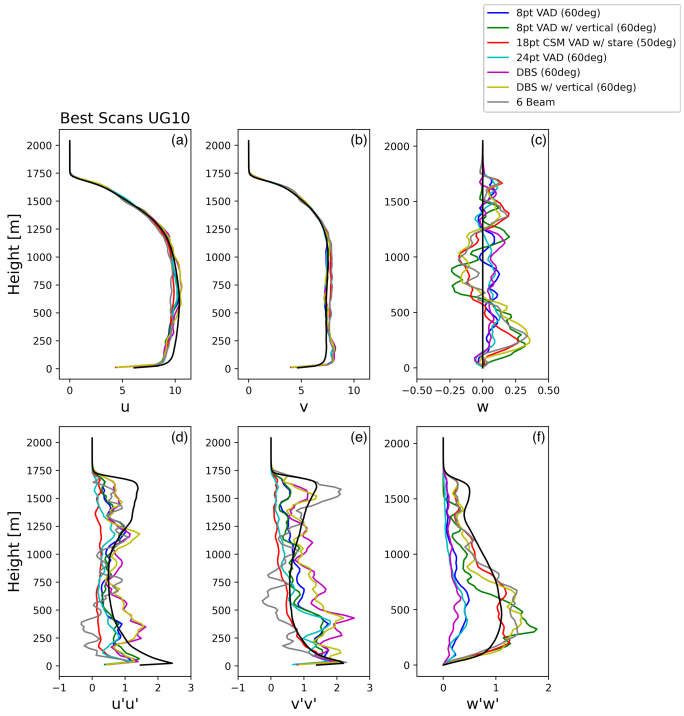

Figure 4. Measured wind values of the most accurate angle from each scanning strategy. The LES mean wind is plotted in black.

Based on mean RMSEs alone, the 8-point VAD with vertical got the best results overall, across all three environments. The 8-point VAD scan without a vertical beam performed the next best overall, followed closely by the 18-point CSM VAD with a staring beam, and then the 24-point VAD. The DBS scan with a vertical beam, the six-beam method, and then finally the DBS all had higher overall averaged RMSEs than the four VAD scans.

The scanning strategy that got the most accurate results from just the UG00 model output, however, is the 8-point VAD. It is followed by the 24-point VAD and DBS scans. The strategy that got the most accurate retrievals from the UG05 and UG10 model outputs is the 8-point VAD with a vertical beam, which as stated above, had the lowest error overall. The 18-point CSM VAD and six-beam method performed second- and third-best based off the UG05 LES output, and the DBS scan with a vertical beam and the six-beam method had the second and third lowest RMSE calculations in the UG10 simulation.

The DBS scanning strategy had the highest error out of all seven scans in the UG05 and UG10 simulations; the UG00 simulation is notably the only one in which it performed quite well in comparison to the other techniques. The DBS scan with a vertical beam, in contrast, got the most accurate mean wind retrievals – as compared to the other scanning methods – in the UG10 LES, and retrieved some of the least accurate measurements from the UG00 and UG05 model outputs.

Figure 4f especially shows a notable difference in the mean vertical variance retrievals between lidar scans which included a vertical beam, and those that did not. This difference can be seen in the w'w' values in Tables 1–3 although, as also shown in the tables, the scans with vertical beams did not get better vertical wind velocity measurements than the scans without. In fact, in the UG00 and UG10 LESs, the scans with vertical beams all had higher errors than the scans without; in the UG05 the scans with vertical beams on average only have a marginally smaller error in mean vertical velocity.

4.2 *Instantaneous Winds and Variances*

The accuracies of the mean wind velocities and variances retrieved by the best scans from each strategy were then verified using

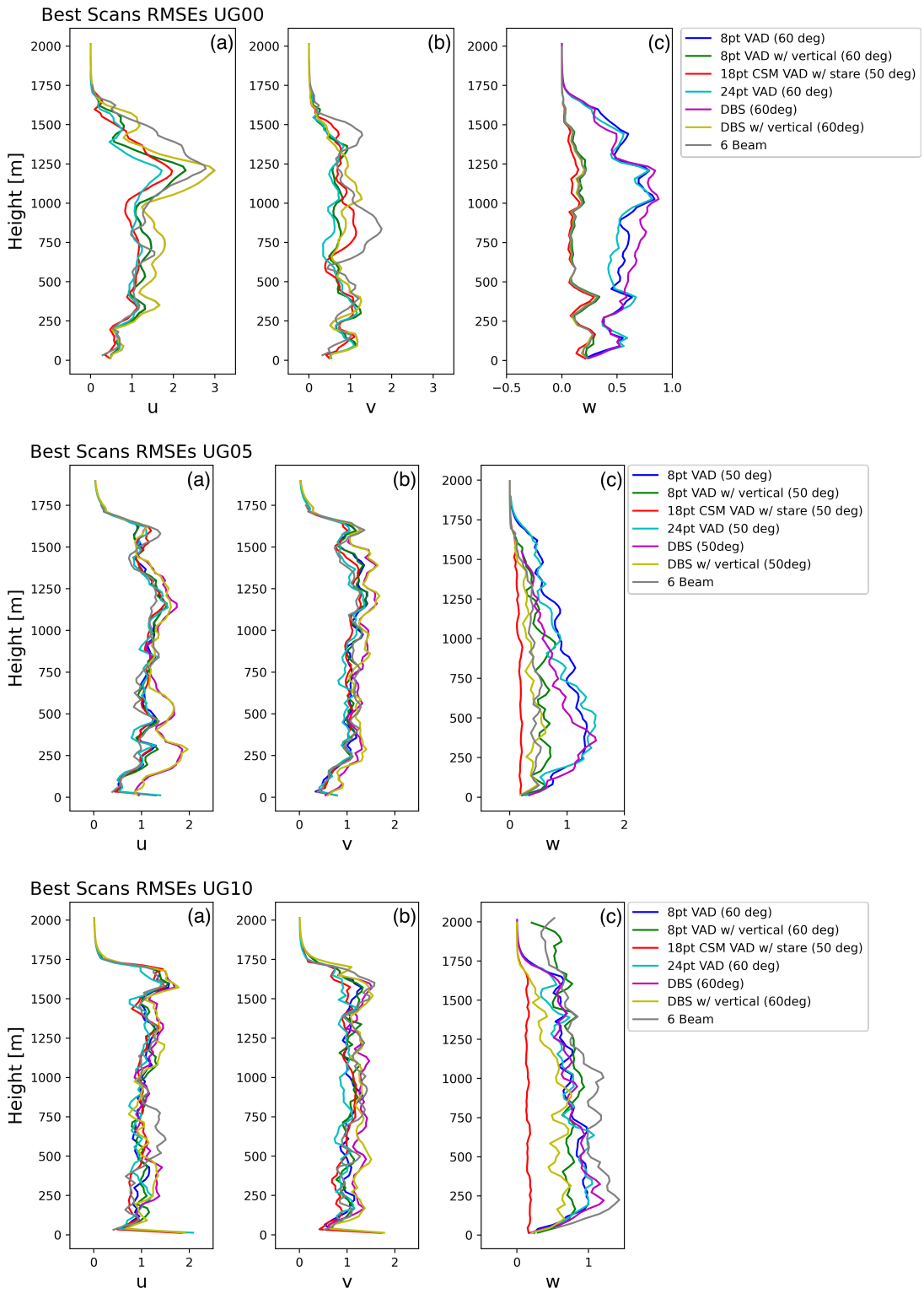

Figure 5. Time-averaged RMSE values of the best elevation angles for each scanning strategy in the UG00, UG05, and UG10 LESs. The RMSEs of the u wind components are plotted in graphs (a), the v components in graphs (b), and the w components in graphs (c).

Table 1. RMSEs for the UG00 simulation. The scan with the lowest error for each velocity and variance component is highlighted in green.

Scanning strategy	U	V	W	U'U'	V'V'	W'W'
8pt VAD (60deg)	0.885	0.238	0.407	0.373	0.381	0.918
8pt VAD w/ vertical (60deg)	0.882	0.240	0.610	0.373	0.382	0.832
18pt CSM VAD w/ stare (50deg)	0.841	0.384	0.610	0.585	0.422	0.838
24pt VAD (60deg)	0.811	0.234	0.415	0.458	0.412	0.936
DBS (60deg)	1.063	0.321	0.281	0.334	0.343	0.833
DBS w/ vertical (60deg)	1.062	0.320	0.610	0.333	0.343	0.833
6Beam	0.982	0.623	0.610	0.558	0.391	0.835

Table 2. RMSEs for the UG05 simulation.

Scanning strategy	U	V	W	U'U'	V'V'	W'W'
8pt VAD (60deg)	0.156	0.213	0.139	0.283	0.276	0.740
8pt VAD w/ vertical (60deg)	0.152	0.219	0.104	0.276	0.286	0.282
18pt CSM VAD w/ stare (50deg)	0.153	0.203	0.112	0.280	0.365	0.270
24pt VAD (60deg)	0.157	0.202	0.137	0.287	0.394	0.764
DBS (60deg)	0.664	0.367	0.107	0.400	0.272	0.803
DBS w/ vertical (60deg)	0.667	0.365	0.099	0.400	0.281	0.282
6Beam	0.144	0.164	0.105	0.416	0.590	0.275

Table 3. RMSEs for the UG10 simulation.

Scanning strategy	U	V	W	U'U'	V'V'	W'W'
8pt VAD (60deg)	0.471	0.298	0.059	0.472	0.495	0.512
8pt VAD w/ vertical (60deg)	0.468	0.307	0.159	0.449	0.476	0.271
18pt CSM VAD w/ stare (50deg)	0.475	0.355	0.114	0.723	0.567	0.138
24pt VAD (60deg)	0.433	0.272	0.063	0.620	0.589	0.551
DBS (60deg)	0.437	0.325	0.064	0.459	0.669	0.591
DBS w/ vertical (60deg)	0.440	0.311	0.151	0.462	0.601	0.214
6Beam	0.488	0.387	0.125	0.692	0.422	0.186

the instantaneous winds measured by the lidar at all heights and at every time between 0 and 600 seconds. This was done to ensure that each of the lidar scans were getting consistently accurate wind retrievals, and that the mean wind values were not misleading.

Figure 5 shows the RMSEs of the instantaneous winds measured by each scanning strategy at every height in the simulations, averaged over time. In Figure 5c it is clear that the scanning methods with vertical beams consistently get lower errors, and therefore are retrieving wind velocities closer to the models' true winds, than the scans without vertical beams in the w direction. Thus, the instantaneous wind measurements confirm that the lidar scans that include a vertical beam got vertical turbulence measurements that were much closer to the actual variance values.

The scans with vertical beams, however, get u and v component wind errors comparable to those of the scans without vertical beams. In the UG00 LES especially, the differences between the 8-point VAD and the 8-point VAD with a vertical beam, as well as between the DBS and the DBS with a vertical beam scans, are negligible. These results indicate that a vertical beam is only necessary in a lidar scan when retrieving accurate instantaneous vertical velocity and turbulence values.

5. CONCLUSIONS

Under the conditions of this experiment, the scanning strategies that were tested with more than one elevation angle generally got the most accurate wind measurements from the 60° and 50° angle scans. Although they each did slightly better or worse depending on the initial wind shears of the test environments, these two elevation angles together got the best overall results as compared to the rest of the angles used. These results indicate that either 60° or 50° will be the most effective elevation angle for measuring winds with a lidar VAD or DBS scan.

The best scans from each strategy that did not include a vertical beam – the 8-point VAD, the 24-point VAD, and the DBS scans – all significantly underestimated average vertical variance in particular. Those scanning strategies that did include a vertical beam – the 8-point VAD with a vertical beam, the 18-point CSM VAD with a staring lidar, the DBS with a vertical beam, and the six-beam method – measured vertical variances

that were much closer to the actual values as given by the LES output. This shows that it is difficult to get accurate measurements for vertical turbulence without including a vertical beam in the lidar scan. The instantaneous variance retrievals confirmed this.

The 18-point continuous scan VAD with a staring lidar, as shown in Tables 2 and 3, got the vertical variance values with the least amount of error in both the UG05 and UG00 simulations. This was as expected since the staring lidar was able to make measurements with a 90° beam for the entire time the lidars were running, as opposed to scans that included a vertical beam but only used one lidar and therefore could not get constant vertical measurements. However, in both those simulations, the CSM VAD with a stare only yielded marginally better vertical turbulence results than the six-beam method; in both cases it also got less accurate vertical wind velocity measurements than the 8-point VAD with a vertical beam and the 8-point VAD, respectively. In the UG00 LES it was outperformed by the DBS scan and the 8-point VAD with a vertical beam scan, which got the vertical velocity and vertical variance values with the least amounts of error. These results suggest that, when making vertical wind observations, a separate staring lidar does not offer a significant advantage over an added vertical beam in a scanning strategy.

The six-beam method, whose unique variance calculations were designed to get more accurate wind turbulence measurements, did a decent job overall. While the strategy got some of the worst measurements for variance in the u and v directions (save for the UG10 LES, where it notably got the best v variance retrieval out of any other scanning technique), its vertical variance measurements all have quite small errors across all three models. However, as evident in Figures 4d and 4e, the six-beam method may also calculate negative u and v variance values. These variances are physically impossible and therefore must be disregarded.

Judging the results from this study as a whole, the VAD scans all did a much better job than the DBS scans at retrieving accurate measurements for wind velocities and turbulence. Therefore, it can be concluded that the greater number of data points collected by the VAD lidar scans makes up for their slower scanning time; a DBS scanning method will give quicker results while a VAD scan will give more accurate ones.

As shown in Tables 1–3 as well as Figure 4, the 8-point VAD with a vertical beam scanning strategy specifically will yield wind measurements that are on average the closest to the environment's true winds. Although, based also on Tables 1–3, different lidar scanning strategies will each give comparatively good results for certain component wind velocities or variances, and comparatively bad results for others. There is no one strategy that will always give the best possible observations for every single value; this dilemma is compounded by the fact that the accuracy of scans varies depending on the elevation angle used and the wind conditions of the environment.

Future studies may benefit from testing the scanning strategies with a wider range of environments. The LESs used in this experiment did not go beyond an initial vertical wind shear of ten meters per second, so doing further tests in simulations with greater wind shears will help to get a clearer idea on how a lidar would perform in real-life boundary layer environments of similar conditions. The test simulations also had a constant stability, so more scans need to be done to observe how a change in that factor will affect the accuracy of turbulence retrievals. The data from this experiment was limited by the 10-minute time period that the lidar scans were run for, as well; continued work can help to verify the results with data collection periods closer to 30 minutes or longer.

6. ACKNOWLEDGMENTS

The author would like to thank Dr. Joshua Gebauer and Dr. Jeremy Gibbs for their guidance and support on this project. This material is based upon work supported by the National Science Foundation under Grant No. AGS-2050267. The statements, findings, conclusions, and recommendations are those of the author(s) and do not necessarily reflect the views of the National Science Foundation, NOAA, or the U.S. Department of Commerce.

7. REFERENCES

Gebauer, J., 2022: LidarSim. GitHub, accessed 21 July 2022, https://github.com/jgebauer44/LidarSim.git.

Lundquist, J.K., M.J. Churchfield, S. Lee, and A. Clifton, 2015: Quantifying error of lidar and sodar Doppler beam swinging measurements of wind turbine wakes using computational

fluid dynamics. *Atmos. Meas. Tech.*, **8**, 907–920, https://doi.org/10.5194/amt-8-907-2015.

Menke, R., N. Vasiljević, J. Wagner, S.P. Oncley, and J. Mann, 2020: Multi-lidar wind resource mapping in complex terrain. *Wind Energ. Sci.*, **5**, 1059–1073, https://doi.org/10.5194/wes-5-1059-2020.

Newman, J.F., P.M. Klein, S. Wharton, A. Sathe, T.A. Bonin, P.B. Chilson, and A. Muschinski, 2016: Evaluation of three lidar scanning strategies for turbulence measurements. *Atmos. Meas. Tech.*, **9**, 1993–2013, https://doi.org/10.5194/amt-9-1993-2016.

Newsom, R.K., C. Sivaraman, T.R. Shippert, and L. Riihimaki, 2019: Doppler Lidar WIND Value-Added Product. DOE ARM Climate Research Facility, Washington, DC (United States), accessed 25 July 2022, https://doi.org/10.2172/1238069.

Robey, R. and J. K. Lundquist, 2022: Behavior and Mechanisms of Doppler Win Lidar Error in Varying Stability Regimes. *Atmos. Meas. Tech.* Discuss. [preprint], https://doi.org/10.5194/amt-2022-73, in review.

van Heerwaarden, C.C., B.J.H. van Stratum, T. Heus, J.A. Gibbs, E. Fedorovich, and J.P. Mellado, 2017: MicroHH 1.0: a computational fluid dynamics code for direct numerical simulation and large-eddy simulation of atmospheric boundary layer flows. *Geosci. Model Dev.*, **10**, 3145–3165, https://doi.org/10.5194/gmd-10-3145-2017.